water

MDPI

Communication

Highly Efficient Reduction of Vanadium (V) with Histidine

Hao Peng [1,*], Laixin Wang [2], Wenjing Pan [1], Sisi Yang [1], Jingjing Wang [1], Jielin Qin [1], Lihua Ao [1], Yinhe Lin [1] and Jinzhu Tang [3,*]

[1] Chongqing Key Laboratory for New Chemical Materials of Shale Gas, College of Chemistry and Chemical Engineering, Yangtze Normal University, Fuling, Chongqing 408100, China
[2] Intelligent Development Department, Huatian Engineering and Technology Corporation, MCC, Nanjing 210000, China; wanglaixinustb@163.com
[3] Green Intelligence Environmental School, Yangtze Normal University, Chongqing 408100, China
* Correspondence: cqupenghao@126.com (H.P.); tangjinzhu11@163.com (J.T.)

Abstract: In this paper, histidine was applied to treat vanadium-containing wastewater. Several independent experimental parameters, including H_2SO_4 concentration, dosage of histidine, reaction time and reaction temperature, were investigated and optimized through response surface methodology. The influence on the reduction process decreased in the following order: dosage of histidine > reaction temperature > reaction time. The reduction efficiency could be achieved at 95.77% under the following reaction conditions: H_2SO_4 concentration of 0.2 mol/L, reaction temperature of 90 °C, dosage of histidine at n(His)/n(V) = 3.6, reaction time of 60 min and stirring rate at 500 rpm. The reduction kinetics was followed successfully with the pseudo-first-order kinetics model and the *Ea* for reduction of vanadium was calculated to be 25.31 kJ/mol. The reduction kinetics was affected by these factors and the kinetics model could be described by an Equation. This paper provides a versatile strategy for treatment of wastewater containing V(V) and shows a bright tomorrow for wastewater treatment.

Keywords: response surface methodology; histidine; reduction; vanadium

check for updates

Citation: Peng, H.; Wang, L.; Pan, W.; Yang, S.; Wang, J.; Qin, J.; Ao, L.; Lin, Y.; Tang, J. Highly Efficient Reduction of Vanadium (V) with Histidine. *Water* **2024**, *16*, 2227. https://doi.org/10.3390/w16162227

Academic Editor: Stefano Papirio

Received: 5 July 2024
Revised: 27 July 2024
Accepted: 5 August 2024
Published: 7 August 2024

Copyright: © 2024 by the authors. Licensee MDPI, Basel, Switzerland. This article is an open access article distributed under the terms and conditions of the Creative Commons Attribution (CC BY) license (https://creativecommons.org/licenses/by/4.0/).

1. Introduction

Vanadium is a critical rare metal playing a pivotal role in various sectors [1–5]. However, excessive exposure to vanadium is harmful to life and leads to issues like pulmonary tumors, kidney lesions, and nervous system damage at higher concentrations [6–9]. A large amount of vanadium-containing wastewateris produced during the vanadium-producing process, some of which might be distributed to the soil or groundwater and threaten the environment [10–14]. Vanadium is an environmental hazardous element according to the United Nations Environment Programme, and the minimum concentration is limited to 0.2 μg/L [15], while the concentrations of vanadium in wastewater collected from Chengde, China, ranged from 0.05 to 0.2 g/L, and 0.076 to 0.208 mg/L in Panzhihua, China [16–20]. Hence, efforts should be made to prevent it.

Nowadays, many techniques are available for vanadium removal, including adsorption [21,22], chemical reduction and precipitation [17,23], ion exchange [24,25], microbial reduction [26–28], biological remediation [14,29–35] and electrochemical reduction [36,37]. Some of these will produce vanadium-containing solid waste, from which utilization as a source of vanadium is not environmentally friendly and unfeasible. Multiple valences of vanadium, including 0, II, III, IV and V, exist in the environment, and vanadium in V is the most mobile, toxic species [38–41]. Commonly, the reduction of vanadium is proven to be an efficient technology for detoxifying vanadium in groundwater, because vanadium atlow-valence is harmless [15,42]. Chemical reduction is one of the most promising methods due to its high efficiency and easy operation.

In this paper, histidine is applied to treat vanadium-containing wastewater, during which histidine is actually used to reduce vanadium rather than just precipitate vanadium.

The experimental parameters (concentration of H_2SO_4, dosage of histidine, reaction temperature and reaction time) of the reduction process are investigated. Response surface methodology (RSM) was used to optimize the reaction conditions and order the influences of the parameters on the reduction process. Reduction kinetics behavior is also analyzed with the pseudo-first-order kinetics model.

2. Materials and Methods

2.1. Materials

The main components, included Na_3VO_4 and $C_6H_9N_3O_2$ (collected from Shanghai Aladdin Biochemical Technology Co., Ltd., Shanghai, China), were used directly.

2.2. Experimental Procedure

For the reduction experiment, a series of experiments was conducted. Firstly, the vanadium solution was prepared by dissolving a certain amount of Na_3VO_4 in deionized water. Then, 100 mL 0.05 M Na_3VO_4 solution was added to a 250 mL beaker placed in a thermostatic water bath with a temperature precision of ±0.1 °C. After the reaction temperature was heated to a predetermined temperature, amounts of $C_6H_9N_3O_2$(n(His)/n(V) = 0.6–3.6) and H_2SO_4(0.1–0.4 mol/L) were added to the above vanadium solution and stirred well. A total of 2 mL of the sample were collected every 10 min and the concentration of vanadium (V) in the sample was measured and determined by ICP–OES [43–45]. Each experiment was conducted three times to ensure the accuracy of the data. The reduction efficiency (η) was calculated via Equation (1):

$$\eta = \frac{C_0 - C_t}{C_0} \times 100\% \quad (1)$$

where C_0 and C_t, are the concentrations of vanadium (V) at initial and time t, respectively, in mg/L.

2.3. Response Surface Optimization

The interactions are ignored in the above experiments, and optimal reaction conditions cannot be determined. Thus, RSM is applied to solve the problem [45–48]. In this paper, response surface methodology (RSM)conducted by Design Expert 8.0 software was applied to optimize the experimental process and order the significance of the experimental parameters. The experimental parameters affecting the reduction process were selected as A (reaction temperature), B (reaction time) and C (n(His)/n(V)), and the reduction efficiency of vanadium was selected as the response. The independent variables and factor levels are detailed in Table 1.

Table 1. Independent variables and factor levels.

Independent Variable	Unit	Level		
		−1	**0**	**1**
A: reaction temperature	°C	30.00	60.00	90.00
B: reaction time	min	10.00	35.00	60.00
C: n(His)/n(V)	-	0.60	2.10	3.60

3. Results

3.1. Single Factor Experiments

The existing forms of vanadium in wastewater were closely related to the pH and concentration of vanadium in wastewater, and their existing forms greatly influenced the reduction process of vanadium. The effect of the H_2SO_4concentrationon the vanadium reduction process was studied experimentally. During the reduction process, the concentrations used were 0.1, 0.2, 0.3 and 0.4 mol/L.

Figure 1 shows that the change in the concentration of H_2SO_4 had a great influence. When the concentration of H_2SO_4 was 0.1 mol/L, the reduction efficiency of vanadium increased along with the dosage of histidine, and the reduction efficiency increased from 40.81% to 74.63%. Although the reduction of vanadium could be enhanced by increasing H_2SO_4 concentration, the reduction efficiency of vanadium decreased gradually with increasing H_2SO_4 concentrations. When the dosage of histidine was set to n(His)/n(V) = 3.6 and the concentration of sulfuric acid was 0.2 mol/L, the greatest reduction efficiency reached 95.77%. When the concentration of H_2SO_4 was low, the pH of the solution was high, and vanadium mainly existed in the anionic form of metavanadate or pyro-vanadate. At this time, the redox ability of vanadium was weak, and it was not easy to reduce to low valence. With increasing H_2SO_4 concentration, the oxidation ability of vanadium gradually increased, and vanadium was easily reduced to a low valence by a reducing agent. With the continuous increase in the concentration of H_2SO_4, pentavalent vanadium easily hydrolyzed at high temperature, which was not conducive to the reduction of vanadium. Therefore, 0.2 mol/L was confirmed as the best concentration for further experiments.

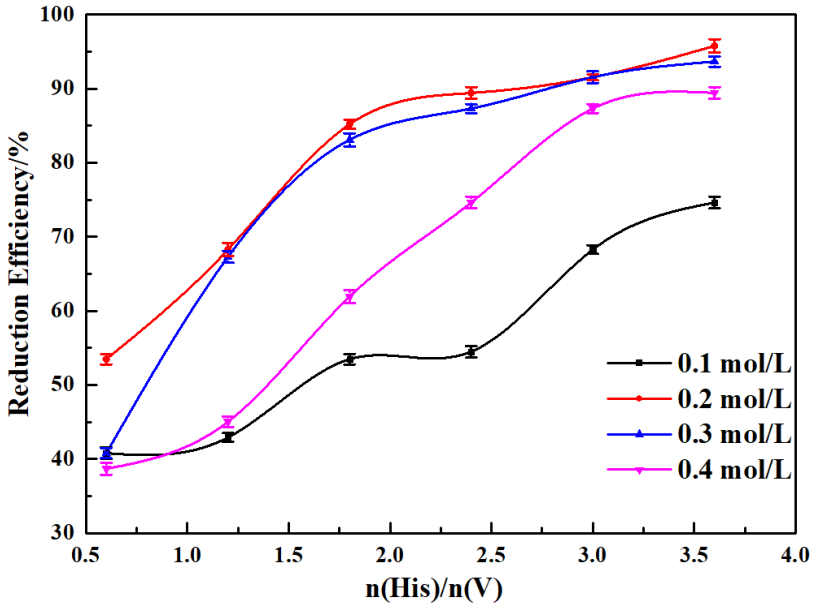


Figure 1. Effect of the H_2SO_4 concentration on the reduction efficiency of vanadium.

From the results shown above, it could be seen that the dosage of histidine also had a significant impact on the reduction efficiency. The influence of the dosage of histidine on the reduction efficiency of vanadium was studied. During the reduction process, the dosage of histidine (n(His)/n(V)) was set to 0.6, 1.2, 1.8, 2.4, 3.0 and 3.6.

Figure 2 shows that, with increasing histidine dosage, the reduction efficiency also increased significantly. The reduction efficiency increased with histidine dosage in both low-temperature and high-temperature media. When the reaction temperature was 30 °C and the dosage of histidine was n(His)/n(V) = 0.6, the reduction efficiency increased from 11.22% to 20.73% as the reaction time increased from 10 min to 60 min, while the increase was slow and insignificant. When the dosage of histidine increased to n(His)/n(V) = 3.6, the reduction efficiency increased from 34.15% to 54.59% as the reaction time increased from 10 min to 60 min, and the total reduction rate increased by 22.93 and 33.86%, respectively. The reduction efficiency increased more obviously at high temperatures. When the reaction temperature was 90 °C and the dosage of histidine was n(His)/n(V) = 0.6, the reduction efficiency increased from 34.47% to 53.49% as the reaction time increased from 10 min to 60 min. When the dosage of histidine was n(His)/n(V) = 3.6, the reduction efficiency increased from 52.32% to 95.77% as the reaction time increased from 10 min to 60 min, and the total reduction efficiency increased by 17.65 and 42.28%, respectively. With the increase in the dosage of histidine and the concentration of reactants, the number of

reactive compounds in the system increased gradually, which promoted the reaction and strengthened the reduction of vanadium. Therefore, n(His)/n(V) = 3.6 was selected.

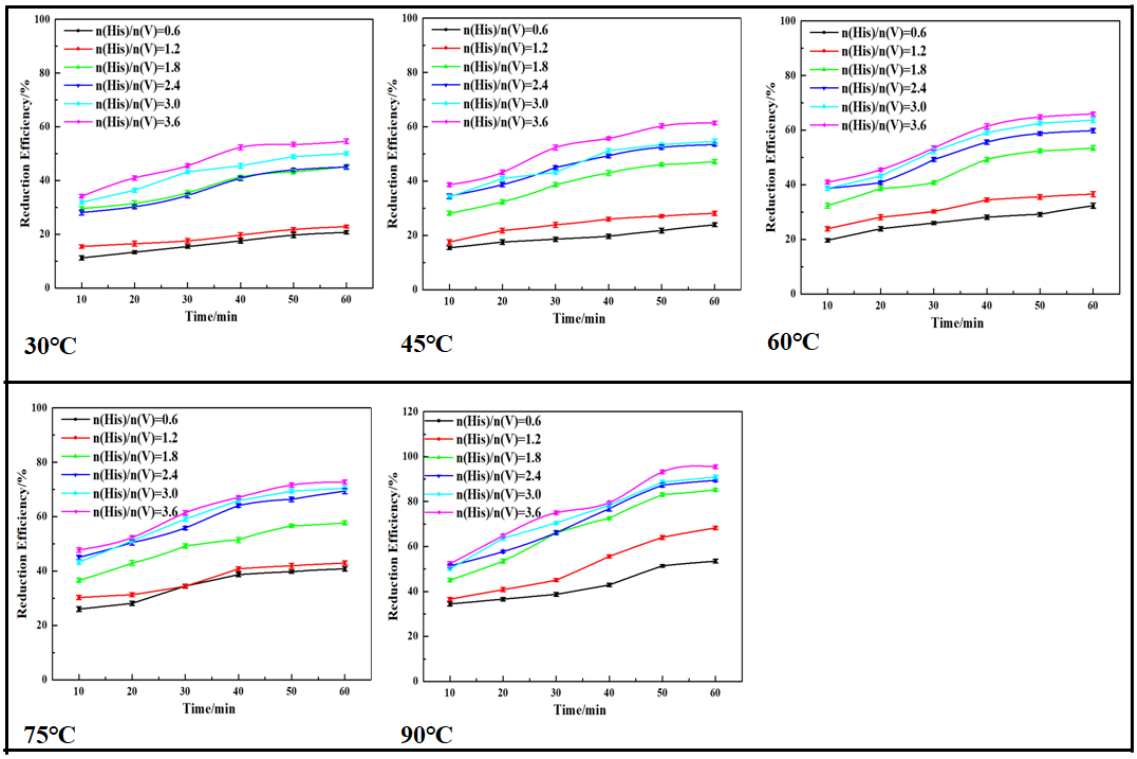


Figure 2. Effect of the dosage of histidine on the reduction efficiency of vanadium.

As an important factor in the chemical reaction process, reaction temperature affected the viscosity and activity of reactants and had a very important influence on the chemical reaction process. The effect of the reaction temperature on the vanadium reduction process was studied. During the reduction process, the reaction temperatures were set to 30 °C, 45 °C, 60 °C, 75 °C and 90 °C.

Figure 2 indicated that the reduction efficiency of vanadium significantly improved with increasein reaction temperature, regardless of whether the amount of histidine was small or large. When the dosage of histidine was n(His)/n(V) = 0.6, the reduction efficiency increased from 20.73% to 53.49% as the reaction temperature increased from 30 °C to 90 °C, which was an increase of 32.76%. With increasing histidine dosage, the influence of the reaction temperature was further strengthened. When the dosage of histidine was n(His)/n(V) = 3.6, the reduction efficiency of vanadium increased from 54.59% to 95.73% as the reaction temperature increased from 30 °C to 90 °C, which was an improvement of 41.14%. With increasing temperature, the movement rate of vanadium ions and histidine in the reaction system was accelerated, the reactivity increased and the viscosity of the solution decreased, hence increasing the reaction rate and the contact between vanadium ions and histidine, which contributed to accelerating the reduction process and improving the reduction efficiency.

Above all, it was concluded that increasing the dosage of histidine, raising the reaction temperature and prolonging the reaction time could enhance the reduction process and improve the reduction efficiency. When the reaction temperature was 90 °C, H_2SO_4 concentration was 0.2 mol/L, the dosage of histidine was n(His)/n(V) = 3.6, the reaction time was 60 min, and the reduction efficiency of vanadium reached 95.77%. Otherwise, the reaction conditions investigated above are suitable for simulated vanadium-containing wastewater and, for real wastewater or industrial application, the reaction conditions should be optimized.

3.2. Response Surface Methodology

To better describe the simulated results, the natural log model (shown in Equation (S6)) was applied:

$$Ln\,(\eta) = 3.90 + 0.35 \times A + 0.25 \times B + 0.41 \times C + 0.021 \times A \times B - 0.090 \times A \times C - 0.000055 \times B \times C + 0.027 \times A^2 - 0.030 \times B^2 - 0.28 \times C^2 \quad (2)$$

According to the results shown in Equation (2), the coefficients for each factor were 0.35 (reaction temperature), 0.25 (reaction temperature) and 0.41 (dosage of histidine) and the positive coefficients corresponded to a positive effect. The detailed interaction of parameters was discussed in the Supporting Information, and the results indicated that RSM (shown in Figure 3) was an effective statistical tool for optimizing the reaction conditions. The influence on the reduction process decreased in the following order: dosage of histidine > reaction temperature > reaction time.

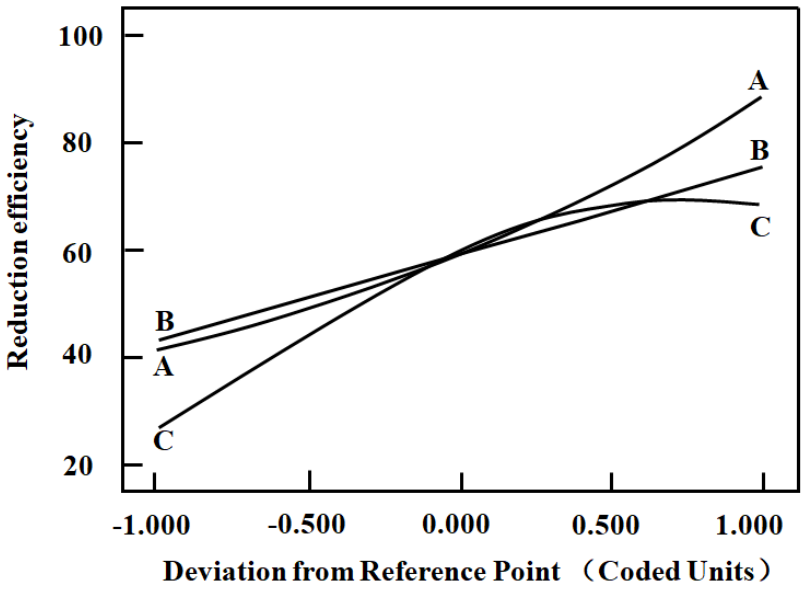


Figure 3. Perturbation plot for the reduction efficiency of vanadium (A, reaction temperature; B, reaction time; C, n(His)/n(V)).

The reduction process of vanadium using histidine through various variables could be investigated through these model equations. Different parameters, R^2, p values, F values and adjusted R^2 values, were measured as standards that were helpful for determining the accuracy of every coefficient to evaluate the significance of the predicted model. The ANOVA results (shown in Table 2) confirmed that the Model F value of 118.63 implies that the model is significant. There is only a 0.01% chance that a large "Model F Value" could occur due to noise. Values of "*Prob* > *F*" less than 0.0500 indicated that the model terms are significant. In this case, A, B, C, AC, and C^2 are significant model terms. The R^2 value reflected how much variability in the observed response values could be expressed by the experimental factors, as well as their interactions, by establishing a relationship between the predicted and experimental results. An R^2 close to one revealed good fitting of the experimental data to the predicted model equation. The regression model produced a higher R^2 of up to 0.9935, signifying excellent fit between the model and the experimental data. The Predicated-R^2 of up to 0.8958 was in reasonable agreement with the adjusted R^2 of 0.9851. Adequate precision was helpful for evaluating the signal-to-noise ratio. A ratio greater than 4 was desirable. Here, a higher adequate precision of 40.991 revealed an adequate signal. This regression model could be applied to navigate the design space.

Table 2. Analysis of variance (ANOVA) for the response.

Source	Sum of Squares	*Df*	Mean Square	*F* Value	*p* Value *Prob > F*
Model	3.14	9	0.35	118.63	<0.0001
A	0.96	1	0.96	324.93	<0.0001
B	0.50	1	0.50	169.78	<0.0001
C	1.32	1	1.32	448.08	<0.0001
A × B	0.001743	1	0.001743	0.59	0.4666
A × C	0.032	1	0.032	10.97	0.0129
B × C	0.00012	1	0.00012	0.041	0.8456
A × A	0.00315	1	0.00315	1.07	0.3352
B × B	0.00384	1	0.00384	1.30	0.2909
C × C	0.32	1	0.32	110.26	<0.0001
Residual	0.021	7	0.00294	-	-
Lack-of-fit	0.021	3	0.00686	-	-
Pure error	0.000	4	0.000	-	-
Cor Total	3.16	16			

3.3. Reduction Kinetics Analysis

The reduction behavior kinetics was analyzed by the pseudo-first-order model (shown in Equation (3)) [49–52].

$$v = \frac{dC}{dt} = -KC \quad (3)$$

Integrate.

$$-LnC = Kt - LnC_0 \quad (4)$$

Firstly, the reducing data were fitted with Equation (4) and the related results were summarized in Table 3. The R^2 values were calculated as 0.9694, 0.9832, 0.9818, 0.9869 and 0.9673, respectively, which were all close to 1, indicating that the pseudo-first-order model was reasonable for simulating the reduction behavior kinetics. Meanwhile, the *Ea* of the reduction process was 25.31 kJ/mol based on the Arrhenius equation as in Equation (5) (shown in Figure 4a). This was far less than the reduction with oxalic acid [53], which indicated that the reduction of vanadium was easier.

$$LnK = LnA - Ea/RT \quad (5)$$

Table 3. Apparent rate constants K correlation coefficients.

Temperature (*K*)	*K* ($min^{-1}K^{-1}$)	R^2
303	0.00773	0.9694
318	0.00988	0.9832
333	0.01214	0.9818
348	0.01420	0.9869
363	0.02824	0.9673

The reduction process was significantly affected by the experimental parameters according to the results analyzed above. To further understand the reduction kinetics behavior, the pseudo-first-order model, Arrhenius equation and the reaction factors (H_2SO_4 concentration [H_2SO_4], dosages of histidine [n(His)/n(V)] and reaction temperatures [T]) were combined in analysis (shown in Equation (6)).

$$K = K_0 \cdot [H_2SO_4]^a \cdot [n(His)/n(V)]^b \cdot [T]^c \cdot exp(-Ea/RT) \cdot t \quad (6)$$

After transformation, Equation (7) was obtained:

$$-LnC = K_0 \cdot [H_2SO_4]^a \cdot [n(His)/n(V)]^c \cdot exp(-Ea/RT) \cdot t - LnC_0 \quad (7)$$

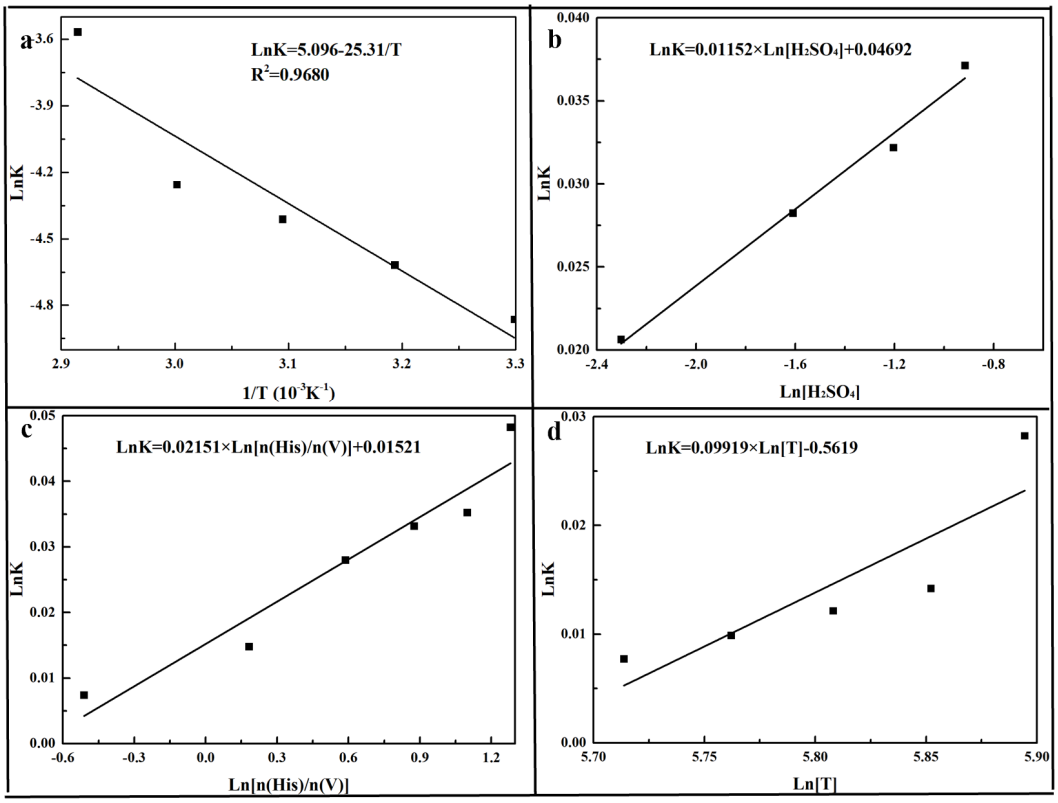


Figure 4. Kinetics plots: (**a**) Arrhenius equation; (**b**) Ln K vs. $[H_2SO_4]$; (**c**) Ln K vs. n(His)/n(V); (**d**) Ln K vs. [T].

All the experimental data were fitted and the results are shown in Table 4 and Figure 4b–d. The exponent orders in Equation (8) were calculated as 0.01152, 0.02151 and 0.09919, respectively. Therefore, the reduction kinetics equation could be described as follows:

$$-LnC = K_0 \cdot [H_2SO_4]^{0.01152} \cdot [n(His)/n(V)]^{0.02151} \cdot [T]^{0.09919} \cdot exp(-25.31/T) \cdot t - LnC_0 \quad (8)$$

Table 4. Apparent rate constants and correlation coefficients for the experimental parameters.

Parameters	*K* (min^{-1}K^{-1})	R^2
$[H_2SO_4]$ (*mol/L*)		
0.1	0.02064	0.9823
0.2	0.02824	0.9673
0.3	0.03218	0.9638
0.4	0.03712	0.9609
n(His)/n(V)		
0.6	0.00738	0.9643
1.2	0.01479	0.9814
1.8	0.02801	0.9896
2.4	0.03319	0.9783
3.0	0.03522	0.9864
3.6	0.04824	0.9673
Temperature (*K*)		
303	0.00773	0.9694
318	0.00988	0.9832
333	0.01214	0.9818
348	0.0142	0.9869
363	0.02824	0.9673

Above all, the results analyzed above showed that histidine was an efficient reductant for treatment of simulated vanadium-containing wastewater, but there is a long way to go before its industrial application. This paper focused only on the reduction behavior of vanadium (V), and some other issues were ignored, including the treatment of products of the oxidation of histidine and reduction products of vanadium (V), high reaction temperature and high concentration of H_2SO_4 used, etc. In the future, the issues mentioned above will be our focus.

4. Conclusions

(1) Histidine was an efficient reductant for vanadium reduction. Increasing the dosage of histidine and raising the reaction temperature could promote the reduction process.

(2) All the experimental factors showed a positive effect on the reduction process and the response surface methodology confirmed that the influence of each parameter on the reduction efficiency decreased in the following order: dosage of histidine > reaction temperature > reaction time. The reduction efficiency of vanadium could be achieved at 95.77% at H_2SO_4 concentration of 0.2 mol/L, the dosage of histidine at n(His)/n(V) = 3.6, reaction temperature of 90 °C, reaction time of 60 min and stirring rate at 500 rpm.

(3) The reduction kinetics was followed with the pseudo-first-order kinetics model with an *Ea* of 25.31 kJ/mol. The reduction kinetics affected by the factors and the kinetics model could be described as follows:

$$-LnC = K_0 \cdot [H_2SO_4]^{0.01152} \cdot [n(His)/n(V)]^{0.02151} \cdot [T]^{0.09919} \cdot exp(-25.31/T) \cdot t - LnC_0$$

Supplementary Materials: The following supporting information can be downloaded at: https://www.mdpi.com/article/10.3390/w16162227/s1, Figure S1: Diagnostic plots of the quadratic model; Figure S2: Response surface plots for factors (X1 = A: Temperature, X2 = B: Time, Actual Factors C: n(His)/n(V) = 0.60, 1.20,1.80, 2.40, 3.00, 3.60); Figure S3: Response surface plots for factors (X1 = A: Temperature, X2 = B: n(His)/n(V), Actual Factors C: Time = 10, 20, 30, 40, 50, 60 min); Figure S4: Response surface plots for factors (X1 = A: Time, X2 = B: n(His)/n(V), Actual Factors C: Temperature = 30, 45, 60, 75, 90 °C).

Author Contributions: Conceptualization, Y.L.; methodology, W.P.; validation, H.P.; formal analysis, J.W.; investigation, J.Q.; data curation, L.A. and S.Y.; writing—original draft preparation, H.P.; writing—review and editing, H.P. and J.T.; visualization, Y.L.; supervision, H.P.; project administration, H.P. and L.W.; funding acquisition, H.P. and L.W. All authors have read and agreed to the published version of the manuscript.

Funding: This work was supported by the key development projects of Liangshan Prefecture (No. 23ZDYF0169 and No. 23ZDYF0173), the National Natural Science Foundation of China (No. U1960101) and Key research and development plan of Anhui Province (No. 2022l07020037) and the Science and Technology Research Program of Chongqing Municipal Education Commission (No. KJQN202201406).

Data Availability Statement: Data are contained within the article.

Conflicts of Interest: Author L. W. was employed by the company Huatian Engineering & Technology Corporation. The remaining authors declare that the research was conducted in the absence of any commercial or financial relationships that could be construed as a potential conflict of interest.

References

1. Mubula, Y.; Yu, M.; Yang, D.; Lin, B.; Guo, Y.; Qiu, T. Recovery of valuable elements from solid waste with the aid of external electric field: A review. *J. Environ. Chem. Eng.* **2023**, *11*, 111237. [CrossRef]
2. Liu, J.; Xing, Z.; Wang, X.; Cheng, G.; Xue, X. Effect of V_2O_5 on Consolidation, Reduction, and Softening-Melting Behavior of High-Cr Vanadium Titanomagnetite. *Metals* **2023**, *13*, 1171. [CrossRef]
3. Bao, S.; Chen, B.; Zhang, Y.; Ren, L.; Xin, C.; Ding, W.; Yang, S.; Zhang, W. A comprehensive review on the ultrasound-enhanced leaching recovery of valuable metals: Applications, mechanisms and prospects. *Ultrason. Sonochem.* **2023**, *98*, 106525. [CrossRef] [PubMed]

4. Shin, K.-H.; Jin, C.-S.; So, J.-Y.; Park, S.-K.; Kim, D.-H.; Yeon, S.-H. Real-time monitoring of the state of charge (SOC) in vanadium redox-flow batteries using UV–Vis spectroscopy in operando mode. *J. Energy Storage* **2020**, *27*, 101066. [CrossRef]
5. Huang, X.; Pu, Y.; Zhou, Y.; Zhang, Y.; Zhang, H. In-situ and ex-situ degradation of sulfonated polyimide membrane for vanadium redox flow battery application. *J. Membr. Sci.* **2017**, *526*, 281–292. [CrossRef]
6. Zhang, B.; Zhang, H.; He, J.; Zhou, S.; Dong, H.; Rinklebe, J.; Ok, Y.S. Vanadium in the Environment: Biogeochemistry and Bioremediation. *Environ. Sci. Technol.* **2023**, *57*, 14770–14786. [CrossRef] [PubMed]
7. Basit, F.; Bhat, J.A.; Alyemeni, M.N.; Shah, T.; Ahmad, P. Nitric oxide mitigates vanadium toxicity in soybean (*Glycine max* L.) by modulating reactive oxygen species (ROS) and antioxidant system. *J. Hazard. Mater.* **2023**, *451*, 131085. [CrossRef]
8. Zwolak, I. Vanadium carcinogenic, immunotoxic and neurotoxic effects: A review of in vitro studies. *Toxicol. Mech. Methods* **2014**, *24*, 1–12. [CrossRef]
9. Jaiswal, M.R.; Kale, P.P. Mini review–vanadium-induced neurotoxicity and possible targets. *Neurol. Sci.* **2020**, *41*, 763–768. [CrossRef]
10. Peng, H.; Yang, L.; Chen, Y.; Guo, J.; Li, B. Recovery and Separation of Vanadium and Chromium by Two-Step Alkaline Leaching Enhanced with an Electric Field and H_2O_2. *ACS Omega* **2020**, *5*, 5340–5345. [CrossRef]
11. Peng, H.; Shang, Q.; Chen, R.; Zhang, L.; Chen, Y.; Guo, J. Step-Adsorption of Vanadium (V) and Chromium (VI) in the Leaching Solution with Melamine. *Sci. Rep.* **2020**, *10*, 6326. [CrossRef] [PubMed]
12. Gilligan, R.; Nikoloski, A.N. The extraction of vanadium from titanomagnetites and other sources. *Miner. Eng.* **2020**, *146*, 106106. [CrossRef]
13. Wen, J.; Jiang, T.; Gao, H.; Zhou, W.; Xu, Y.; Zheng, X.; Liu, Y.; Xue, X. An efficient utilization of chromium-containing vanadium tailings: Extraction of chromium by soda roasting-water leaching and preparation of chromium oxide. *J. Environ. Manag.* **2019**, *244*, 119–126. [CrossRef] [PubMed]
14. Wang, G.; Zhang, B.; Li, S.; Yang, M.; Yin, C. Simultaneous microbial reduction of vanadium (V) and chromium (VI) by Shewanella loihica PV-4. *Bioresour. Technol.* **2017**, *227*, 353–358. [CrossRef]
15. Chen, G.; Liu, H. Understanding the Reduction Kinetics of Aqueous Vanadium(V) and Transformation Products Using Rotating Ring-Disk Electrodes. *Environ. Sci. Technol.* **2017**, *51*, 11643–11651. [CrossRef] [PubMed]
16. Zhang, H.; Li, P.; Zhang, X.; Chen, X.; Liu, W.; Luo, L.; Han, Y.; Fan, B.; Zheng, S.; Wang, Z.; et al. Removal of vanadium and chromium from vanadium wastewaters with amino-functionalized γ-AlOOH. *Hydrometallurgy* **2022**, *210*, 105841. [CrossRef]
17. Kologrieva, U.; Volkov, A.; Krasnyanskaya, I.; Stulov, P.; Wainstein, D. Analysis of Hydrometallurgical Methods for Obtaining Vanadium Concentrates from the Waste by Chemical Production of Vanadium Pentoxide. *Materials* **2022**, *15*, 938. [CrossRef] [PubMed]
18. El-Naggar, A.; Shaheen, S.M.; Chang, S.X.; Hou, D.; Ok, Y.S.; Rinklebe, J. Biochar Surface Functionality Plays a Vital Role in (Im)Mobilization and Phytoavailability of Soil Vanadium. *ACS Sustain. Chem. Eng.* **2021**, *9*, 6864–6874. [CrossRef]
19. Fang, D.; Zhang, X.; Dong, M.; Xue, X. A novel method to remove chromium, vanadium and ammonium from vanadium industrial wastewater using a byproduct of magnesium-based wet flue gas desulfurization. *J. Hazard. Mater.* **2017**, *336*, 8–20. [CrossRef] [PubMed]
20. Cao, X.; Diao, M.; Zhang, B.; Liu, H.; Wang, S.; Yang, M. Spatial distribution of vanadium and microbial community responses in surface soil of Panzhihua mining and smelting area, China. *Chemosphere* **2017**, *183*, 9–17. [CrossRef]
21. Al-Ghouti, M.A.; Ashfaq, M.Y.; Khan, M.; Al Disi, Z.; Da'na, D.A.; Shoshaa, R. State-of-the-art adsorption and adsorptive filtration based technologies for the removal of trace elements: A critical review. *Sci. Total Environ.* **2023**, *895*, 164854. [CrossRef] [PubMed]
22. Peng, H.; Guo, J.; Li, B.; Huang, H.; Shi, W.; Liu, Z. Removal and recovery of vanadium from waste by chemical precipitation, adsorption, solvent extraction, remediation, photo-catalyst reduction and membrane filtration. A review. *Environ. Chem. Lett.* **2022**, *20*, 1763–1776. [CrossRef]
23. Liu, H.; Yang, Q. Study on Precipitation Kinetics of Calcium Pyro-Vanadate and Thermodynamics of Vanadium Water System. *Metals* **2022**, *13*, 10. [CrossRef]
24. Saleh, T.A.; Mustaqeem, M.; Khaled, M. Water treatment technologies in removing heavy metal ions from wastewater: A review, Environmental Nanotechnology. *Monit. Manag.* **2022**, *17*, 100617.
25. Zhu, X.; Li, W.; Zhang, Q.; Zhang, C.; Chen, L. Separation characteristics of vanadium from leach liquor of red mud by ion exchange with different resins. *Hydrometallurgy* **2018**, *176*, 42–48. [CrossRef]
26. Chen, S.; Li, J.; Li, Z.; Li, S.; Zhang, B. Electrical stimulation promotes synchronous nitrobenzene bio-degradation and vanadate bio-reduction. *Chem. Eng. J.* **2023**, *475*, 146119. [CrossRef]
27. Shi, J.; Li, Z.; Zhang, B.; Li, L.; Sun, W. Synergy between pyridine anaerobic mineralization and vanadium (V) oxyanion bio-reduction for aquifer remediation. *J. Hazard. Mater.* **2021**, *418*, 126339. [CrossRef] [PubMed]
28. Hao, L.; Liu, Y.; Chen, N.; Hao, X.; Zhang, B.; Feng, C. Microbial removal of vanadium (V) from groundwater by sawdust used as a sole carbon source. *Sci. Total Environ.* **2021**, *751*, 142161. [CrossRef] [PubMed]
29. Li, Y.; Low, G.K.C.; Scott, J.A.; Amal, R. Microbial reduction of hexavalent chromium by landfill leachate. *J. Hazard. Mater.* **2007**, *142*, 153–159. [CrossRef]
30. Reijonen, I.; Metzler, M.; Hartikainen, H. Impact of soil pH and organic matter on the chemical bioavailability of vanadium species: The underlying basis for risk assessment. *Environ. Pollut.* **2016**, *210*, 371–379. [CrossRef]

31. Suman, N.; Rangabhashiyam, S.; Balasubramanian, P.; Paresh, K. A review of chromite mining in Sukinda Valley of India: Impact and potential remediation measures. *Int. J. Phytoremediation* **2020**, *22*, 804–818.
32. Lin, H.; Liu, J.; Dong, Y.; He, Y. The effect of substrates on the removal of low-level vanadium, chromium and cadmium from polluted river water by ecological floating beds. *Ecotoxicol. Environ. Saf.* **2019**, *169*, 856–862. [CrossRef] [PubMed]
33. Levina, A.; Lay, P.A. Stabilities and Biological Activities of Vanadium Drugs: What is the Nature of the Active Species? *Chem.–Eur. J.* **2017**, *12*, 1692–1699. [CrossRef]
34. Shaheen, S.M.; Rinklebe, J.; Rupp, H.; Meissner, R. Lysimeter trials to assess the impact of different flood–dry-cycles on the dynamics of pore water concentrations of As, Cr, Mo and V in a contaminated floodplain soil. *Geoderma* **2014**, *228–229*, 5–13. [CrossRef]
35. Shaheen, S.M.; Rinklebe, J.; Frohne, T.; White, J.R.; DeLaune, R.D. Redox effects on release kinetics of arsenic, cadmium, cobalt, and vanadium in Wax Lake Deltaic freshwater marsh soils. *Chemosphere* **2016**, *150*, 740–748. [CrossRef]
36. Nancharaiah, Y.V.; Mohan, S.V.; Lens, P.N. Metals removal and recovery in bioelectrochemical systems: A review. *Bioresour. Technol.* **2015**, *195*, 102–114. [CrossRef]
37. Cai, Z.F.; Zhang, Z.M.; Guo, Z.C.; Tang, H.Q. Direct electrochemical reduction of solid vanadium oxide to metal vanadium at low temperature in molten $CaCl_2$-NaCl. *Int. J. Miner. Metall. Mater.* **2012**, *19*, 499–505. [CrossRef]
38. Peng, H.; Guo, J.; Zhang, X. Leaching Kinetics of Vanadium from Calcium-Roasting High-Chromium Vanadium Slag Enhanced by Electric Field. *ACS Omega* **2020**, *5*, 17664–17671. [CrossRef] [PubMed]
39. Mangini, L.F.K.; Valt, R.B.G.; Ponte, M.J.J.d.S.; Ponte, H.d.A. Vanadium removal from spent catalyst used in the manufacture of sulfuric acid by electrical potential application. *Sep. Purif. Technol.* **2020**, *246*, 116854. [CrossRef]
40. Li, H.; Wang, C.; Lin, M.; Guo, Y.; Xie, B. Green one-step roasting method for efficient extraction of vanadium and chromium from vanadium-chromium slag. *Powder Technol.* **2020**, *360*, 503–508. [CrossRef]
41. Huang, X.; Ye, Z.; Chen, L.; Chen, X.; Liu, C.; Yin, Y.; Wang, X.; Wei, Y. Removal of V(V) From Solution Using a Silica-Supported Primary Amine Resin: Batch Studies, Experimental Analysis, and Mathematical Modeling. *Molecules* **2020**, *25*, 1448. [CrossRef]
42. Liu, H.; Zhang, B.; Yuan, H.; Cheng, Y.; Wang, S.; He, Z. Microbial reduction of vanadium (V) in groundwater: Interactions with coexisting common electron acceptors and analysis of microbial community. *Environ. Pollut.* **2017**, *231*, 1362–1369. [CrossRef]
43. Peng, H.; Guo, J. Reduction behavior of chromium(VI) with oxalic acid in aqueous solution. *Sci. Rep.* **2020**, *10*, 17732. [CrossRef] [PubMed]
44. Peng, H.; Leng, Y.; Guo, J. Electrochemical Removal of Chromium (VI) from Wastewater. *Appl. Sci.* **2019**, *9*, 1156. [CrossRef]
45. Peng, H.; Leng, Y.; Cheng, Q.; Shang, Q.; Shu, J.; Guo, J. Efficient Removal of Hexavalent Chromium from Wastewater with Electro-Reduction. *Processes* **2019**, *7*, 41. [CrossRef]
46. Peng, H.; Shang, Q.; Chen, R.; Leng, Y.; Guo, J.; Liu, Z.; Tao, C. Oxidative Leaching Kinetics of Vanadium from the Vanadium-Chromium-Reducing Residue with $K_2Cr_2O_7$. *ACS Omega* **2020**, *5*, 8777–8783. [CrossRef]
47. Peng, H.; Wang, F.; Li, G.; Guo, J.; Li, B. Highly Efficient Recovery of Vanadium and Chromium: Optimized by Response Surface Methodology. *ACS Omega* **2019**, *4*, 904–910. [CrossRef]
48. Zhang, X.; Liu, Z.; Fan, X.; Lian, X.; Tao, C. Optimization of reaction conditions for the electroleaching of manganese from low-grade pyrolusite. *Int. J. Miner. Metall. Mater.* **2015**, *22*, 1121–1130. [CrossRef]
49. Okello, V.A.; Mwilu, S.; Noah, N.; Zhou, A.; Chong, J.; Knipfing, M.T.; Doetschman, D.; Sadik, O.A. Reduction of hexavalent chromium using naturally-derived flavonoids. *Environ. Sci. Technol.* **2014**, *46*, 10743–10751. [CrossRef]
50. Zhang, X.; Fu, W.; Yin, Y.; Chen, Z.; Qiu, R.; Simonnot, M.-O.; Wang, X. Adsorption-reduction removal of Cr(VI) by tobacco petiole pyrolytic biochar: Batch experiment, kinetic and mechanism studies. *Bioresour. Technol.* **2018**, *268*, 149–157. [CrossRef]
51. Chen, G.; Han, J.; Mu, Y.; Yu, H.; Qin, L. Two-stage chromium isotope fractionation during microbial Cr(VI) reduction. *Water Res.* **2019**, *148*, 10–18. [CrossRef] [PubMed]
52. Langeslay, R.R.; Kaphan, D.M.; Marshall, C.L.; Stair, P.C.; Sattelberger, A.P.; Delferro, M. Catalytic Applications of Vanadium: A Mechanistic Perspective. *Chem. Rev.* **2019**, *119*, 2128–2191. [CrossRef] [PubMed]
53. Peng, H.; Tang, D.; Liao, M.; Wu, Y.; Fan, X.; Li, B.; Huang, H.; Shi, W. A Clean Method for Vanadium (V) Reduction with Oxalic Acid. *Metals* **2022**, *12*, 557. [CrossRef]

Disclaimer/Publisher's Note: The statements, opinions and data contained in all publications are solely those of the individual author(s) and contributor(s) and not of MDPI and/or the editor(s). MDPI and/or the editor(s) disclaim responsibility for any injury to people or property resulting from any ideas, methods, instructions or products referred to in the content.